THE GEOLOGICAL SOCIETY OF AMERICA®

Morphometric scaling relationships in submarine channel–lobe systems

Luke Pettinga[1], Zane Jobe[1], Lauren Shumaker[1], and Nick Howes[2]
[1]Department of Geology and Geological Engineering, Colorado School of Mines, Golden, Colorado 80401, USA
[2]Mathworks, 1 Apple Hill Drive, Natick, Massachusetts 01760, USA

ABSTRACT

Morphometric analysis of submarine fan systems, the largest sedimentary deposits on Earth, demonstrates scaling relationships between genetically related channels and lobe-shaped bodies (LBs) deposited beyond the channel terminus, providing insight into the architectural development of these systems. Compiling dimensional data from depositional systems that cover a range of sediment supply characteristics, tectonic settings, and geographic locations enables investigation into global trends in depositional morphology. LBs have a consistent, scale-independent length-to-width ratio of ~2:1. The thickness-to-area ratios for LBs show multiple morphologic trends, likely driven by topographic confinement, with LBs getting proportionally thicker in relation to increasing confinement. Morphometric analysis of genetically related channel dimensions (width, relief, cross-section area) and LB dimensions (length, width, thickness, area, volume) reveals robust scaling relationships; most notably, channel width and cross-sectional area can be used to predict the volume and depositional area of related LBs. These relationships demonstrate that LBs proportionally scale to their concomitant channels, and thus to the volume of sediment supplied prior to an avulsion. While the dimensions of submarine fans scale to associated terrestrial catchments, the building blocks of submarine fans (i.e., channels and LBs) do not, suggesting a down-system decoupling (or lack of scaling) at LB deposition time scales. Applying these morphometric trends and scaling relationships as input parameters for source-to-sink and reservoir models can improve predictions of stratigraphic architecture, sediment partitioning, and sediment/carbon flux in modern and ancient submarine fan systems.

INTRODUCTION

Scaling relationships of sediment-routing systems provide insights into the intrinsic properties and processes of those systems by identifying linkages between morphometric and other quantitative characteristics (e.g., hydraulic properties and sediment flux). For example, scaling relationships have been identified between segments within source-to-sink systems (e.g., Sømme et al., 2009), as well as in finer-scale studies within specific depositional environments (rivers, estuaries, deltas; e.g., Leopold and Langbein, 1962). However, relatively few studies have focused on scaling relationships in submarine fans, which are net-depositional environments within continental-margin sediment-routing systems that are diverse in size and morphology (Fig. DR1 in the GSA Data Repository[1]). These composite depositional features consist of channels and multiple scales of lobe-shaped bodies (LBs), formed by channelized and unconfined sediment gravity flows, respectively (Piper and Normark, 1983). While previous studies have focused on the scaling relationships of submarine channels (e.g., Covault et al., 2012; Reimchen et al., 2016) or LBs (e.g., Jegou et al., 2008; Prélat et al., 2009, 2010), scaling between submarine channels and LBs remains unexplored. In this study of Eocene to modern fan systems, we (1) document the morphometrics of, and scaling relationships between, submarine channels and concomitant (i.e., genetically related) LBs from element to complex scale (i.e., larger than bed scale); (2) evaluate the utility of these relationships for predicting depositional body dimensions in data-poor areas; and (3) investigate potential relationships between terrestrial portions of sediment-routing systems and channel-LB morphology.

DATA AND METHODS

We compiled dimensional data for LBs (n = 271) and, when possible, concomitant channels (n = 52, 160 LBs have paired channel data) from 35 submarine-fan systems (Fig. 1A). The data set of channel and LB measurements made from sonar and seismic-reflection surveys (Fig. 1B) includes submarine-fan systems that cover a range of geographic locations, tectonic settings, source-to-sink configurations, and sediment-supply characteristics (e.g., catchment size; see Table DR1 in the Data Repository), which enables investigation into how system characteristics influence depositional morphology and scaling. Dimensional data from basin floor, slope, and ponded fan settings are included, but we excluded LBs showing evidence of significant sediment bypass (i.e., thoroughgoing channels). Confinement (*sensu* Prélat et al., 2010) at the system scale is documented as 'confined' when basin topography limits the runout of the LBs, or 'unconfined' when LB runout is not significantly impacted by topographic variability or basin margins. We acknowledge that the morphology of individual channel-LB systems changes as they grow (Deptuck et al., 2008); this variability is endemic to our data set, which provides the most comprehensive collection of channel-LB dimensions published to date.

We documented LB dimensions based on facies boundaries and stratal onlap/downlaps (Fig. 1B): the down-flow length (L_{LB}) from the proximal end of the channel-LB transition (a diffuse zone at the channel mouth dominated by erosion and sediment bypass; Wynn et al., 2002) to the distal edge of the LB; the maximum width (W_{LB}) of the LB measured perpendicular to L_{LB};

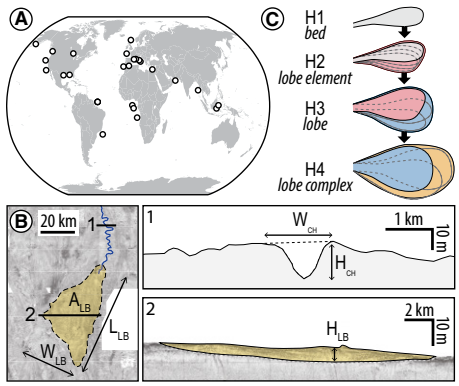

Figure 1. A: Geographic distribution of the 35 submarine fans included in this study. B: Example of measurements made from sonar and seismic data: channel width (W_{CH}) and relief (H_{CH}), and lobe body width (W_{LB}), length (L_{LB}), area (A_{LB}), and thickness (H_{LB}); modified from Jegou et al. (2008). C: Schematic diagram of hierarchy and compensational stacking of lobe bodies (modified from Deptuck et al., 2008).

[1]GSA Data Repository item 2018305, Table DR1 (tabulated data including submarine channel and lobe body dimensions and contextual information) and Figure DR1 (examples of variation in size and geometry of modern submarine fan systems), is available online at http://www.geosociety.org/datarepository/2018/ or on request from editing@geosociety.org.

the maximum depositional thickness (H_{LB}) of the deposit; the total depositional area (A_{LB}) downstream of the channel-LB transition; and LB volume (V_{LB}). Delineating LB boundaries is at times difficult and interpretive due to data quality and gradational facies transitions at the channel-LB transition and LB margins. To mitigate this issue, we focused on high-quality seafloor and near-surface data (typically <100 m subsurface). When direct measurements of A_{LB} and V_{LB} could not be made, we assumed that LBs have an ellipsoid shape to estimate A_{LB} (Equation 1, n = 75) and V_{LB} (Equation 2, n = 198), using an approach similar to Prélat et al. (2009).

$$A_{LB} = \pi \frac{L_{LB}}{2} \frac{W_{LB}}{2} = \frac{1}{4} \pi L_{LB} W_{LB}. \quad (1)$$

$$V_{LB} = \frac{1}{2}\left(\frac{4}{3}\pi \frac{L_{LB}}{2} \frac{W_{LB}}{2} H_{LB}\right)$$

$$= \frac{1}{6} \pi L_{LB} W_{LB} H_{LB}. \quad (2)$$

These equations do not account for the range of LB morphologies, which causes a mean absolute percent error of calculated versus measured A_{LB} and V_{LB} of ~25%. Compensational stacking occurs at multiple scales within LBs, and various hierarchical schemes are used in the literature to describe the resultant deposits (e.g., Deptuck et al., 2008; Prélat et al., 2009; Straub and Pyles, 2012). For consistency, we applied standardized hierarchical terminology to all LBs by qualitatively matching their original documentation to the hierarchy defined by Prélat et al. (2009). This hierarchy consists of four levels (Fig. 1C) in increasing size and complexity: 'beds' (H1) deposited by an individual event/turbidity current; 'lobe elements' (H2) composed of stacked beds/bed sets; 'lobes' (H3) formed by one or more stacked lobe elements fed by a single channel; and 'lobe complexes' (H4) that develop when avulsions or channel migrations result in development of multiple lobes (Prélat et al., 2009). Individual beds (H1) are not included in our analysis due to limited data availability.

We documented channel (not channel belt or complex) dimensions because they represent the conduit through which sediment gravity flows passed prior to forming LBs and thus sediment discharge. Channel measurements included bankfull channel width (W_{CH}), defined here as the distance between levee crests (*sensu* Pirmez and Imran, 2003); channel relief (H_{CH}), the vertical distance between the channel thalweg and the average height of the levee crests; and channel cross-sectional area (A_{CH}), the area between the channel bed and the bankfull surface. Because A_{CH} often decreases downslope (Pirmez and Imran, 2003), channel measurements were made upstream of the transition from channel-to-LB within a streamwise distance of 1–2 L_{LB} of the associated LB (Fig. 1B). We calculated A_{CH} using the assumption that channel cross sections are half-ellipses:

$$A_{CH} = \frac{1}{2} \pi H_{CH} \frac{W_{CH}}{2} = \frac{1}{4} \pi H_{CH} W_{CH}. \quad (3)$$

RESULTS

Morphometrics of Submarine Channels

Submarine channel aspect ratios (W_{CH}/H_{CH}) in this study (median = 44) are consistent with those documented by Konsoer et al. (2013; Fig. 2A; Table DR1). Channel dimensions from this study are generally small compared to those of Konsoer et al., likely because submarine channels typically decrease in size downstream and, unlike Konsoer et al., we exclusively measured distal channel reaches (Fig. 2A).

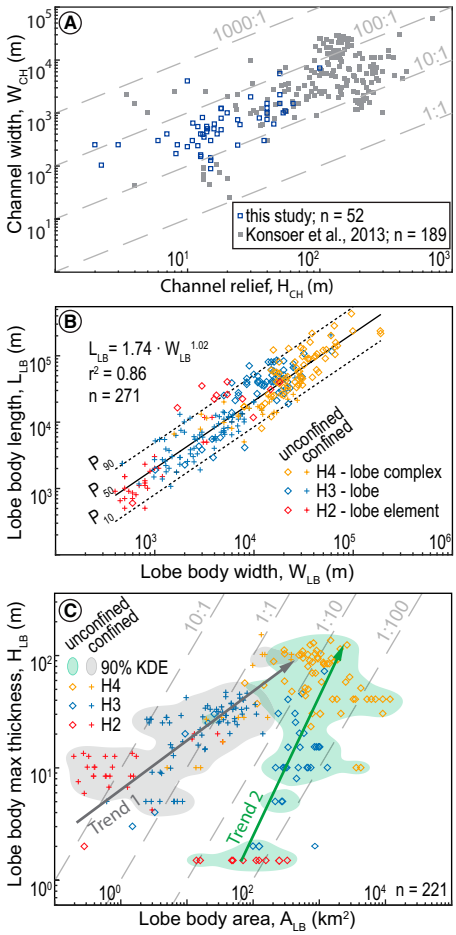

Figure 2. A: Plot of channel width versus channel relief showing consistent ranges of aspect ratios between channels in this study and those of Konsoer et al. (2013). B: Lobe body length versus width shows a strong correlation, with median a length-to-width ratio of ~2:1. C: Lobe body thickness versus area shows two apparent trends in the three-dimensional morphology of lobe bodies (after Prélat et al., 2010). The trends correspond with the distributions of confined and unconfined lobe bodies, illustrated by kernel density estimate (KDE) contours. Aspect ratios are shown as dashed lines in A and C.

Morphometrics of Lobe Bodies

A robust power-law relationship exists for the planform morphology (L_{LB} and W_{LB}) for all LBs ($L_{LB} = 1.74\, W_{LB}^{1.02}$, $r^2 = 0.86$, n = 271) and similar trends exist within each hierarchical level (r^2 values >0.72; Fig. 2B; Table DR1). The planform aspect ratios (L_{LB}/W_{LB}) of LBs demonstrate a relatively narrow range of planform geometries (circular versus elongate), with a median of 2:1 (Fig. 2B; $P_{10} = 1.2$, $P_{50} = 2.0$, $P_{90} = 4.4$). Planform dimensions generally increase from H2 to H4 within individual systems, but considerable overlap between hierarchical levels indicates that their dimensions are not globally consistent (Fig. 2B), likely due to differences in the formative properties (e.g., flow volumes and grain size). There is more than an order-of-magnitude difference between the average volumes of each hierarchical level of LB (H2 = 0.07 km^3, H3 = 2.9 km^3, H4 = 62.0 km^3), similar to the findings of Prélat et al. (2010). However, significant overlap between the dimensions of hierarchical levels indicates that hierarchy cannot be inferred solely from LB dimensions (cf. Prélat et al., 2009).

In contrast to their planform morphology, the three-dimensional (3-D) morphologies of LBs do not show simple scaling. Figure 2C documents the significant variability in the thickness-to-area ratio (H_{LB}/A_{LB}), revealing two trends. Trend 1 illustrates the distribution of confined LBs, which are proportionally thicker than unconfined LBs illustrated in Trend 2. These trends agree with observations of 'lobe' (H3) morphologies made by Prélat et al. (2010), but our data incorporate more hierarchical levels and a wider variety and number of systems. The two trends are distinct at lower A_{LB} values, but converge as A_{LB} increases; accordingly, the trends are identified in H2 and H3, but are indistinguishable for H4. Trend 1 shows a shift to lower H_{LB}/A_{LB} (m/km^2) ratios with increasing area and hierarchy level (from ~10:1 to <1:1), while Trend 2 typically remains between 1:10 and 1:100 (Fig. 2C).

Scaling Relationships between Channels and Lobe Bodies

Our morphometric analysis demonstrates several strong scaling relationships between concomitant channels and LBs. Statistical analysis of channel (W_{CH}, H_{CH}, A_{CH}) and LB (A_{LB}, H_{LB}, V_{LB}) dimensions for hierarchical levels H2–H4 shows that W_{CH} has a strong, positive power-law scaling with both A_{LB} and V_{LB} ($r^2 \approx 0.7$; Fig. 3). A_{CH} also shows a positive, albeit weaker, power-law scaling with both A_{LB} and V_{LB} ($r^2 \approx 0.6$; Fig. 3). H_{CH} does not correlate with any LB dimensions ($r^2 < 0.27$), and no channel dimension correlates with H_{LB} ($r^2 < 0.26$; Fig. 3). Additionally, our investigation of possible relationships between channel-LB dimensions and sediment-routing–system parameters (fluvial catchment area, water discharge, and suspended sediment load) found no significant correlations ($r^2 < 0.35$; Fig. 4).

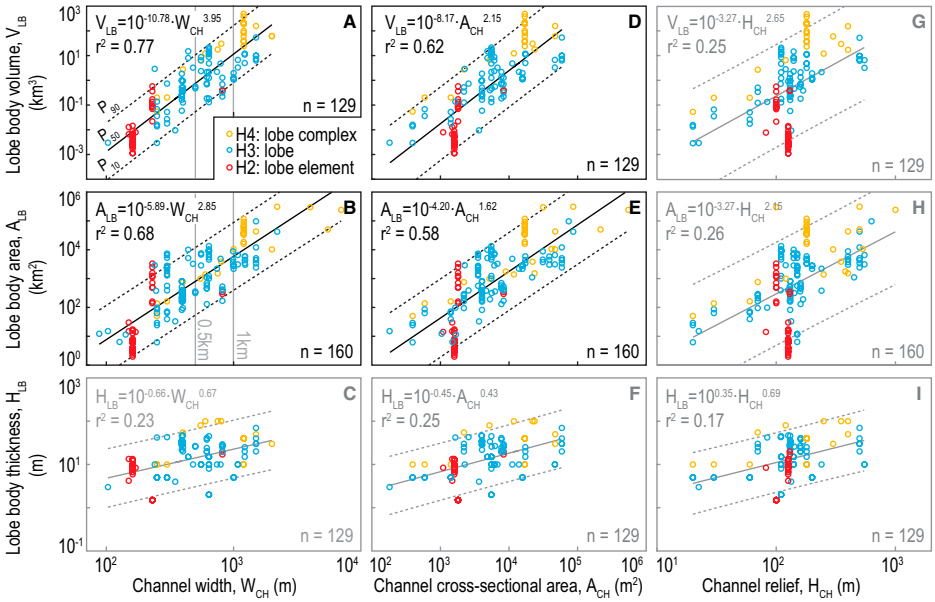

Figure 3. Scaling relationships between some dimensions (A,B,D, and E; black outlines: $r^2 > 0.5$), but not other dimensions (C and F–I; gray outlines: $r^2 < 0.3$), of concomitant channels and lobe bodies. Solid diagonal lines are power-law correlations (P_{50}), and dashed lines show the 80% prediction interval (P_{10}, P_{90}). Channel width and area strongly correlate with both lobe body area and volume, but neither lobe body thickness nor channel relief correlate with any dimensions of associated elements.

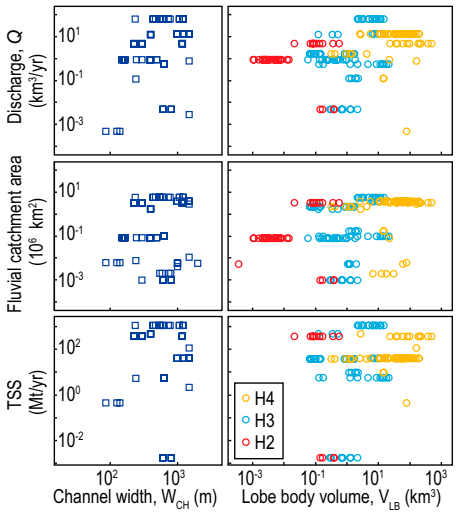

Figure 4. Plots illustrating the absence of correlations between dimensions of the architectural elements of submarine fans (width of distal channel reaches and lobe body volume for hierarchies H2–H4) with parameters of associated terrestrial catchments (Milliman and Farnsworth, 2013): water discharge, fluvial catchment area, and total suspended solids (TSS). The lack of correlation ($r^2 < 0.2$) between these and all other dimensions of channels and lobe bodies in this study (Table DR1 [see footnote 1]) indicates decoupling between the terrestrial and deep-water segments of sediment-routing systems, and/or that autogenic processes may be the primary control on the morphology of submarine channels and lobe bodies.

DISCUSSION

Controls on Morphology and Volume of Lobe Bodies

Planform aspect ratios of LBs display a high degree of consistency across all hierarchical levels (Fig. 2B). Having a strong L_{LB}-W_{LB} relationship in spite of the wide range of system characteristics represented by the data set highlights a potentially universal trend in LB planform geometry, and indicates that turbidity flow properties (rather than external factors) impart primary control on LB planform geometries. This is supported by flume experiments, which show that flow properties (density, volume, sediment type) primarily impact deposit geometry (Baas et al., 2004), while factors that modify the flow processes (e.g., topographic confinement) seem to be secondary (Al Ja'Aidi et al., 2004). The dimensions of LBs change throughout the time span of their deposition, which is dictated by avulsions (Deptuck et al., 2008); accordingly, our measurements of modern, active LBs will underrepresent their final deposit dimensions.

The presence of multiple trends between H_{LB} and A_{LB} (Fig. 2C) indicates that the relative thickness of LBs is more sensitive to external factors. If the impacts of external factors (e.g., confinement) on LB geometry are known, it is possible to predict H_{LB}-A_{LB} relationships using the trends in Figure 2C. While flow properties such as sediment grain size and concentration impact sediment dispersal, and thus LB thickness (Baas et al., 2004), our data demonstrate that topographic confinement strongly influences the 3-D morphology of LBs (Fig. 2C; also see Covault and Romans 2009; Prélat et al., 2010). When unconfined, flows spread out to produce thin LBs with relatively large depositional areas, but when confined, the depositional areas of flows are limited, resulting in LBs with greater relative thickness (Al Ja'Aidi et al., 2004).

Additionally, the two trends in Figure 2C have different implications for the dependence of compensational stacking on V_{LB} and/or the hierarchical level of LBs. Straub and Pyles (2012) suggest that compensational stacking should cause reduced H_{LB}/A_{LB} ratios with increased hierarchical level. Confined systems (Trend 1) in Figure 2C align with Straub and Pyles's (2012) prediction; however, unconfined systems (Trend 2) have a relatively consistent H_{LB}/A_{LB} ratio regardless of LB volume or hierarchical level. If confinement is indeed driving the trends in Figure 2C, the impact of compensational stacking on deposit morphology is variable across LB hierarchies in confined systems, but consistent in unconfined systems.

Controls on Channel-Lobe Body Scaling

W_{CH} and A_{CH} have strong scaling relationships with A_{LB} and V_{LB} (Fig. 3). The lack of correlations between the vertical measurements (H_{CH}, H_{LB}) and other parameters of channel-LB systems may stem from basin confinement (as discussed above) as well as the lower relative accuracy of vertical (thickness, relief) measurements (Fig. 3). The data in this study support a simple association between turbidite flow properties, channel morphology, and lobe dimensions. Because the hydraulic geometries of submarine channels are proportional to their formative sediment-gravity-flow events (Konsoer et al., 2013) and V_{LB} is proportional to the dimensions of the associated channel (Fig. 3), accordingly, V_{LB} is proportional to the properties of the LB-forming sediment gravity flows (e.g., volume and number of flows).

Submarine-fan dimensions scale with associated catchment parameters (Sømme et al., 2009), but this study indicates that the dimensions of channels and LBs that comprise fans do not (Fig. 4). We did not find any significant correlations between terrestrial catchment parameters (area, water discharge, and suspended sediment load) and submarine channel or LB dimensions (Fig. 4). While these relationships exist when comparing catchments to overall fan dimensions (Sømme et al., 2009), our data suggest that, at smaller spatiotemporal scales (i.e., LB deposition over 10^2–10^4 yr; Deptuck et al., 2008; Jegou et al., 2008), the terrestrial and submarine portions of these systems are decoupled due to autogenic processes (e.g., avulsion) and incomplete transfer of sediment (Romans et al., 2016).

Predicting Channel and Lobe Body Dimensions

Scaling relationships between submarine channels and LBs (Figs. 3A, 3B, 3D, and 3E) provide a tool for predicting the dimensions of these sedimentary features, if the scale of one

parameter is known (e.g., from subsurface seismic data). Figure 5 contains predicted ranges of A_{LB} and V_{LB} for channels with widths of 0.5 km and 1.0 km, using Figures 3A and 3B. Data limitations do not allow direct prediction of hierarchical levels of LB dimensions; however, because LB dimensions generally increase with hierarchy, H2 through H4 LBs should successively fall between P_{10} to P_{90} for a given channel dimension in Figure 3. This information is valuable because hierarchical level influences the architectural complexity of LBs (Pyrcz et al., 2005). Channel-LB scaling provides insight into the sedimentation dynamics that generate the depositional architecture of submarine fans; however, when applying these relationships to ancient systems, differences between active channel conduits and channel-fill deposits must be addressed. The lack of correlations involving H_{CH} or H_{LB} in Figure 3 may stem from their natural variability due to knickpoint migration in channels and antecedent topography for LBs, or the relatively low precision of vertical versus lateral measurements.

CONCLUSIONS

This study documents morphometric trends for lobe bodies in submarine fans, scaling relationships between concomitant submarine channels and LBs, and decoupling of sedimentary processes and fluxes between key parameters of submarine channel-LB deposits and associated terrestrial drainages. LBs have consistent planform length-width relationships ($L_{LB} = 1.74 W_{LB}^{1.02}$; $r^2 = 0.86$, n = 271) and a restricted range of planform aspect ratios (length/width): P_{10} = 1.2, P_{50} = 2.0, P_{90} = 4.4. There are two trends in the 3-D morphology of LBs: (1) LBs that form in topographically confined settings tend to have higher maximum thickness/area ratios that decrease with increased scale, and (2) LBs that form in topographically unconfined settings tend to have lower and hierarchy-independent maximum thickness/area ratios. While distinct for lower hierarchical levels, these trends converge and become indistinguishable at higher hierarchical levels. We interpret that topographic confinement is the primary driver of the thickness/area trends of LBs, but additional factors (e.g., grain size) may also influence these trends.

Submarine channel width and cross-sectional area show power-law scaling with both the depositional area and volume of concomitant LBs. The relationship between channel width and LB volume ($V_{LB} = 10^{-10.78} \cdot W_{CH}^{3.95}$; $r^2 = 0.77$) indicates that (1) channel dimensions scale to the total volume of sediment that passes through the channel before an avulsion or shift in the location of deposition causes a new LB to be established, and (2) LBs scale to the volumes of turbidite flows passing through channels. Applications of these dimensional ranges and scaling relationships include providing realistic input parameters for source-to-sink modeling of sediment budgets, and reservoir models for natural-resource characterization. The lack of correlations between terrestrial catchment-scale parameters and channel-LB dimensions suggests decoupling of sediment fluxes/processes between the terrestrial and deep-water portions of sediment routing systems.

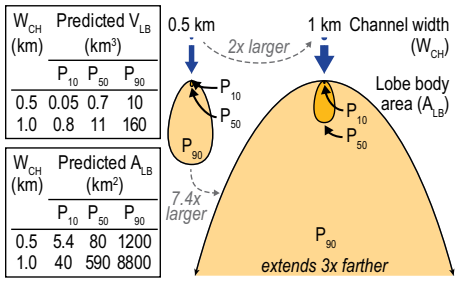

Figure 5. Predicted dimensions of lobe body volume (V_{LB}) and area (A_{LB}) for channel widths (W_{CH}) of 0.5 and 1 km based on formulas in Figures 3A and 3B. The visual representation of the predicted range of A_{LB} for 0.5- and 1-km-wide channels demonstrates that a 2× increase in channel width results in a 7.4× increase in predicted A_{LB} .

ACKNOWLEDGMENTS

Financial support for this work was provided by Chevron Corporation to the Chevron Center of Research Excellence at the Colorado School of Mines (USA). This paper benefited from discussions with Ashley Harris, Fabien Laugier, Jeremiah Moody, and Morgan Sullivan. This manuscript benefited substantially from reviews by Ian Kane, Amandine Prélat, Tor Sømme, an anonymous reviewer, and editor James Schmitt.

REFERENCES CITED

Al Ja'Aidi, O.S., McCaffrey, W.D., and Kneller, B.C., 2004, Factors influencing the deposit geometry of experimental turbidity currents: Implications for sand-body architecture in confined basins, *in* Lomas, S.A., and Joseph, P., eds., Confined Turbidite Systems: Geological Society of London Special Publications, v. 222, p. 45–58, https://doi.org/10.1144/GSL.SP.2004.222.01.04.

Baas, J.H., van Kesteren, W., and Postma, G., 2004, Deposits of depletive high-density turbidity currents: A flume analogue of bed geometry, structure and texture: Sedimentology, v. 51, p. 1053–1088, https://doi.org/10.1111/j.1365-3091.2004.00660.x.

Covault, J.A., and Romans, B.W., 2009, Growth patterns of deep-sea fans revisited: Turbidite-system morphology in confined basins, examples from the California Borderland: Marine Geology, v. 265, p. 51–66, https://doi.org/10.1016/j.margeo.2009.06.016.

Covault, J.A., Shelef, E., Traer, M., Hubbard, S.M., Romans, B.W., and Fildani, A., 2012, Deep-water channel run-out length: Insights from seafloor geomorphology: Journal of Sedimentary Research, v. 82, p. 21–36, https://doi.org/10.2110/jsr.2012.2.

Deptuck, M.E., Piper, D.J.W., Savoye, B., and Gervais, A., 2008, Dimensions and architecture of late Pleistocene submarine lobes off the northern margin of East Corsica: Sedimentology, v. 55, p. 869–898, https://doi.org/10.1111/j.1365-3091.2007.00926.x.

Jegou, I., Savoye, B., Pirmez, C., and Droz, L., 2008, Channel-mouth lobe complex of the recent Amazon Fan: The missing piece: Marine Geology, v. 252, p. 62–77, https://doi.org/10.1016/j.margeo.2008.03.004.

Konsoer, K., Zinger, J., and Parker, G., 2013, Bankfull hydraulic geometry of submarine channels created by turbidity currents: Relations between bankfull channel characteristics and formative flow discharge: Journal of Geophysical Research: Earth Surface, v. 118, p. 216–228, https://doi.org/10.1029/2012JF002422.

Leopold, L., and Langbein, W., 1962, The Concept of Entropy in Landscape Evolution: U.S. Geological Survey Professional Paper, v. 500-A, 20 p.

Milliman, J.D., and Farnsworth, K.L., 2013, River Discharge to the Coastal Ocean: A Global Synthesis: Cambridge, UK, Cambridge University Press, 394 p.

Piper, D.J.W., and Normark, W.R., 1983, Turbidite depositional patterns and flow characteristics, Navy Submarine Fan, California Borderland: Sedimentology, v. 30, p. 681–694, https://doi.org/10.1111/j.1365-3091.1983.tb00702.x.

Pirmez, C., and Imran, J., 2003, Reconstruction of turbidity currents in Amazon Channel: Marine and Petroleum Geology, v. 20, p. 823–849, https://doi.org/10.1016/j.marpetgeo.2003.03.005.

Prélat, A., Hodgson, D.M., and Flint, S.S., 2009, Evolution, architecture and hierarchy of distributary deep-water deposits: A high-resolution outcrop investigation from the Permian Karoo Basin, South Africa: Sedimentology, v. 56, p. 2132–2154, https://doi.org/10.1111/j.1365-3091.2009.01073.x.

Prélat, A., Covault, J.A., Hodgson, D.M., Fildani, A., and Flint, S.S., 2010, Intrinsic controls on the range of volumes, morphologies, and dimensions of submarine lobes: Sedimentary Geology, v. 232, p. 66–76, https://doi.org/10.1016/j.sedgeo.2010.09.010.

Pyrcz, M.J., Catuneanu, O., and Deutsch, C.V., 2005, Stochastic surface-based modeling of turbidite lobes: AAPG Bulletin, v. 89, p. 177–191, https://doi.org/10.1306/09220403112.

Reimchen, A.P., Hubbard, S.M., Stright, L., and Romans, B.W., 2016, Using sea-floor morphometrics to constrain stratigraphic models of sinuous submarine channel systems: Marine and Petroleum Geology, v. 77, p. 92–115, https://doi.org/10.1016/j.marpetgeo.2016.06.003.

Romans, B.W., Castelltort, S., Covault, J.A., Fildani, A., and Walsh, J.P., 2016, Environmental signal propagation in sedimentary systems across timescales: Earth-Science Reviews, v. 153, p. 7–29, https://doi.org/10.1016/j.earscirev.2015.07.012.

Sømme, T.O., Helland-hansen, W., Martinsen, O.J., and Thurmond, J.B., 2009, Relationships between morphological and sedimentological parameters in source-to-sink systems: A basis for predicting semi-quantitative characteristics in subsurface systems: Basin Research, v. 21, p. 361–387, https://doi.org/10.1111/j.1365-2117.2009.00397.x.

Straub, K.M., and Pyles, D.R., 2012, Quantifying the hierarchical organization of compensation in submarine fans using surface statistics: Journal of Sedimentary Research, v. 82, p. 889–898, https://doi.org/10.2110/jsr.2012.73.

Wynn, R.B., Kenyon, N.H., Masson, D.G., Stow, D.A.V., and Weaver, P.P.E., 2002, Characterization and recognition of deep-water channel-LB transition zones: AAPG Bulletin, v. 8, p. 1441–1462.

Manuscript received 10 May 2018
Revised manuscript received 19 July 2018
Manuscript accepted 22 July 2018

Printed in USA